

Article

Geochemical Equilibrium Modelling of the Aqueous Speciation of Select Trace Elements in the Great Lakes

John Fitzgerald, Colton Bentley and Bas Vriens * 

Department of Geological Sciences & Engineering, Queen's University, Kingston, ON K7L 2N8, Canada

* Correspondence: bas.vriens@queensu.ca

Abstract: The behaviour and fate of trace elements in surface waters are greatly affected by their chemical form in solution, but the aqueous speciation of dissolved trace elements in the North American Great Lakes has received relatively little attention. Here, we present results from geochemical equilibrium modelling with 2021 surface water quality data to examine the spatiotemporal dynamics of trace element speciation in the Great Lakes. The relative abundance of aqueous trace element species appeared consistent with variability in solution chemistry and followed basin-wide trends in pH, alkalinity, salinity, and nutrient levels. The speciation of alkali metals was dominated by free monovalent cations, and that of oxyanion-forming elements by oxoacids, whereas significant fractions (>1%) of other aqueous complexes were also evident for rare earth elements (e.g., Ce and Gd as carbonates), alkaline earth metals (e.g., Sr as sulfates), or transition metals (e.g., Zn as phosphates). Spatially, differences in the relative abundance of aqueous trace element species were <2 orders of magnitude, with the highest variation (~50-fold) occurring for select chloride-complexes, resulting from upstream-to-downstream salinity increases in the basin. Finally, simulations of various future water quality scenarios (e.g., decreasing P levels, increasing temperature and salinity) suggest that the speciation of most trace elements is robust temporally as well. This study demonstrates how considering aqueous speciation may help improve the understanding of trace element dynamics and support water quality management in the Great Lakes.

Keywords: Great Lakes; trace elements; surface water quality; geochemical equilibrium modelling



Citation: Fitzgerald, J.; Bentley, C.; Vriens, B. Geochemical Equilibrium Modelling of the Aqueous Speciation of Select Trace Elements in the Great Lakes. *Water* **2023**, *15*, 1483. <https://doi.org/10.3390/w15081483>

Academic Editor: Dimitrios E. Alexakis

Received: 22 March 2023

Revised: 6 April 2023

Accepted: 8 April 2023

Published: 11 April 2023



Copyright: © 2023 by the authors. Licensee MDPI, Basel, Switzerland. This article is an open access article distributed under the terms and conditions of the Creative Commons Attribution (CC BY) license (<https://creativecommons.org/licenses/by/4.0/>).

1. Introduction

Sustainable management of surface water quality requires a quantitative understanding of the prevailing physicochemical conditions and biogeochemical processes that control the occurrence and behaviour of aqueous solutes, including nutrients, major ions, and trace elements, as well as potential pollutants. The different sources and processes affecting the occurrence and fate of these compounds render water quality monitoring efforts expensive, particularly in large-scale systems, and complicate long-term predictions of changing water quality as a result of anthropogenic emissions, policy implementation, or climate change [1,2]. The North American Great Lakes are a uniquely important but also complex environmental system, with sea-like physical characteristics due to their size, yet with a chemical composition typical of freshwaters [3,4]. The lakes have a long history of anthropogenic pollution, particularly in the so-called Areas of Concern, which has led to implementation of water quality monitoring programs to support management decisions to improve and protect water quality [5]. Important aspects of these monitoring efforts include the mapping of physical properties and concentrations of solutes, notably nutrients, major ions, and emerging contaminants [3,5–7]. While past programs have been successful in expanding our knowledge base on the underlying dynamics driving the Great Lakes water quality and informing subsequent policies to reduce environmental degradation, important knowledge gaps persist [8–10]. Among these is an understanding

of the processes governing the spatial distribution and temporal variability in trace element concentrations [10–12].

Previous [13–15] as well as more recent studies [16–18] have investigated the trace element distribution patterns in the Great Lakes. These works have implicated various factors contributing to the observed trace element dynamics, including inputs from upstream connecting channels, riverine and surface runoff, and atmospheric deposition, as well as loss of certain solutes due to biological uptake and sedimentation. These controlling factors differ over time as well as across the basin [18], i.e., from the oligotrophic Lake Superior to mesotrophic waters in Western Lake Erie [19]. Yet, the role of aqueous speciation (i.e., the distribution of a chemical element amongst all its possible dissolved compounds) in explaining the spatiotemporal occurrence patterns of many trace elements remains unclear, even though the aqueous speciation may significantly impact the propensity of solutes to be biologically scavenged or to interact with, or adsorb to, settling particulates [20–22]. Because of its role in explaining the mobility and fate of trace elements, a quantitative understanding of the aqueous speciation of trace elements in the Great Lakes is thus important.

Geochemical equilibrium modelling presents a powerful tool to examine the aqueous partitioning of chemical elements among valence states, dissolved ions and neutral molecules, hydrolysis products, and aqueous complexes, as well as their occurrence as or association with pure minerals, solid solutions, gases, or surface complexes [23]. Modelling of elemental speciation is used for a wide variety of environmental and geological problems, e.g., mineral-fluid interactions and solute mobility in porous media and in groundwater, or in the unsaturated zone and surface water systems [24,25]. Geochemical equilibrium modelling software such as the Geochemist's Workbench, MINEQL+ [26] and PHREEQC [27] is widely used in industry and academia alike. However, the efficacy of geochemical equilibrium modelling is dependent on many factors, particularly the choice of model database [28,29] and its elemental coverage of the required thermodynamic constants, and their properties and reactions of concern [30]. A persistent challenge is that robust thermodynamic data pertaining to the redox, hydrolysis and aqueous complexation reactions and surface interactions of trace elements remains scarce relative to those for major ions and nutrients [31]. Furthermore, the suitability of equilibrium simulations is limited for disequilibrium systems, where geochemical reactions may be kinetically controlled [32]. Therefore, equilibrium modelling is preferably applied to problems requiring analysis on time scales far exceeding those of the reactions considered (e.g., oxidation-reduction or mineral dissolution reactions). The fact that transport times in the Great Lakes are on the order of years to decades (hydraulic residence times range between 2 years for Lake Erie to 190 years for Lake Superior [33], and many trace metals have residence times of >10 days [13]) make this system suited for geochemical equilibrium modelling of aqueous speciation.

As such, we have applied geochemical equilibrium modelling to explore the aqueous speciation of select trace elements in surface waters in the Great Lakes basin. We leverage recent major and trace element concentration data for the Great Lakes [10] and an expanded thermodynamic database to understand spatial patterns and distribution trends of trace elements across the basin and to examine potential shifts in trace element speciation under various scenarios for water quality changes in the Great Lakes, including warming, salinification, and changes to nutrient loads.

2. Methods and Materials

2.1. Water Quality Data Selection

Surface water quality data for the five Great Lakes connecting channels (upstream-to-downstream: St. Mary's River, St. Clair River, Detroit River, Niagara River, and St. Lawrence River) measured in 2021 were adopted from [10] for physicochemical parameters (temperature, pH, Eh, alkalinity, and specific conductance) and trace and major element concentrations, and from [3,6,34] for the long-term average concentration of additional major elements. All water quality data was collected from epilimnion and stream samples from <1 m depth and represent total dissolved concentrations (operationally defined as

the fraction $<0.22 \mu\text{m}$ or $0.45 \mu\text{m}$ by membrane filtration) and included data for individual aqueous species (total dissolved alkalinity/carbonate, sulfate, chloride, total dissolved phosphate) as well as total dissolved elemental concentrations. Concentrations of dissolved organic matter (DOM) were adopted from [35,36], while other aqueous solutes, including nitrogen and halogen elements other than Cl, were not considered.

All abovementioned water quality parameters and concentrations were arithmetically averaged across sampling locations within each connecting channel system for 2021 (applicable to data from [10]) or for the most recent annual monitoring cycle (applicable to data from [3,6,34]) to establish the aggregate ranges of water chemistry across the basin. For the data adopted from [10], measurements below their respective limits of detection were considered to be half of the respective detection limit. The final averages and ranges of the water quality parameters and concentrations that were adopted for further equilibrium modelling are summarized in Table S1 in the Supplementary Materials.

2.2. Geochemical Equilibrium Modelling Approach

The focus of this work is equilibrium modelling of aqueous trace element speciation, and therefore, the constructed simulations did not consider gaseous or solid phases (i.e., mineral precipitation, adsorption), transport, or (kinetically defined) biological processes. Estimates of total suspended solids (TSSs) in the Great Lakes indicate suspended particulate levels may be significant in certain (nearshore) areas but less in the connecting channels (rough ranges between 1 and 5 mg L^{-1} ; [6,35]) and certainly lower than the total dissolved solids (TDSs) levels ($>100 \text{ mg L}^{-1}$ for the former; [3]). While biological processing of aqueous solutes may strongly affect water chemistry, e.g., through nutrient uptake or changes in dissolved oxygen or pH, it was assumed that such effects on the trace element speciation are predominantly indirect, i.e., through changes in solution chemistry in terms of major ions and not active trace element uptake. Furthermore, it was reasoned that inclusion of explicit kinetic terms for biological uptake would introduce an unnecessary model complexity with associated challenges in parameterization (overfitting), despite the fact that the lack of biological controls may impact speciation dynamics.

The open-access software PHREEQC version 3.7.3-15968 [27] was used for geochemical equilibrium modelling. The Minteq.v4 database, derived from MINTEQA2 version 4 [37] provided with PHREEQC, was used after the addition of select speciation definitions that were adopted from the LLNL database (thermo.com.V8.R6.230) and the BRGM (French Geological Survey, Orléans, France) Thermoddem databases (e.g., for Ge, Nb, Pt, and Rh; [38]). Dissolved organic matter (DOM) was approximated through stoichiometric conversion of dissolved organic carbon (DOC) as glucose using data adopted from both [35,36] that showed DOC ranges from 1000 to $2800 \mu\text{g L}^{-1}$ between the St. Marys and St. Lawrence Rivers, respectively. Because of the large number of aqueous parameters, and major and trace element concentrations ($n > 50$) considered in the geochemical models, the discussion of simulated trends in aqueous speciation is mostly focused on a selection of 8 trace elements: the alkaline earth metals Li and Rb, the oxyanion-forming transition metal V and non-metal Se, the transition metals Mn and Ni, and the rare earth elements Ce and Gd. These elements were selected because they could consistently be measured in all samples and span a range of possible aqueous complexation behaviour under the conditions studied. Table 1 summarizes the coverage of the aqueous speciation of these trace elements of interest achieved by the modified thermodynamic database. Additional settings for the surface water simulations included fixed pH, pe, and dissolved oxygen directly adopted from the in-situ field measurements (i.e., no fixed equilibrium with the atmospheric partial oxygen pressure), and default water pressure and density. For quality control, the ion charge balance for the simulated surface waters was investigated and contrasted to ionic strength, specific conductance and the analytical uncertainty associated with the adopted water quality parameters.

Table 1. Aqueous speciation coverage in the modified database for select trace elements.

	Redox States	Carbonate Complexes	Halogen Complexes	Sulfate Complexes	Phosphate Complexes	Major Cations	Minor Cations
Li	{1}	N/A	Cl	Included	N/A	N/A	N/A
Rb	{1}	N/A	Cl, Br, I	Included	N/A	N/A	N/A
Mn	{0, 2, 3, 6}	Included	F, Cl	Included	Included	N/A	N/A
Ni	{2}	N/A	Cl, Br	Included	Included	N/A	N/A
V	{2, 3, 4, 5}	N/A	F	Included	Included	Fe, K, Ca, Mg	Mn
Se	{−2, 4, 6}	N/A	N/A	N/A	N/A	Ca, Cu, Fe, K, Mg, Na	Cd, Co, Mn, Ni, Zn, Ba, Cd, Pb, Li, Mn, Ag, Sn, Sr, Th
Gd	{2, 3, 5}	Included	F, Cl	Included	Included	N/A	N/A
Ce	{2, 3, 4}	Included	F, Cl, Br, I	Included	Included	N/A	N/A

2.3. Sensitivity Analysis and Extrapolations

In addition to the equilibrium modelling aimed at resolving spatial trends in water chemistry across the Great Lakes, simulations were performed to assess the potential variability in trace element speciation under projected scenarios of future water quality extrapolated until 2100. The following scenarios were examined (the ranges of extrapolated parameter values are summarized in Table S2):

1. Temperature: Long-term average seasonal variability in surface water temperatures in the Great Lakes ranges from 0 °C to 16 °C in Lake Superior and from 0 °C to 24 °C in Lake Erie (<https://coastwatch.glerl.noaa.gov/statistic/> (accessed on 1 December 2022)). Surface waters in the Great Lakes are further expected to warm at a rate of ~0.5 °C per decade [39]. To reflect both seasonal and long-term variability, simulations were performed with connecting channel water temperatures up to 10 degrees below and above the average water temperatures recorded in 2021 (Table S1; [18]).
2. Salinity: All the Great Lakes are experiencing increasing salinification [3,40]. Previously assessed regression analysis on a long-term Cl concentration time-series for each of the Great Lakes presented in [41] were extrapolated to 2100 for their downstream connecting channels examined here, and the predicted Cl concentrations were adopted directly (Table S2).
3. Alkalinity: Previous longitudinal analysis of a carbonate alkalinity time-series for each of the Great Lakes between 1965–2005 revealed increasing levels in Lakes Superior and Huron yet decreasing levels in Lakes Erie and Ontario [3]. The average (linear) rates of change over that time period were extrapolated to 2100 and predicted alkalinity concentrations were adopted directly (Table S2).
4. Phosphate: Analysis of phosphorus (P) dynamics in the Great Lakes surface waters has revealed a large spatiotemporal variation of phosphate levels [19], well-beyond what was recorded in the connecting channel waters in 2021 (Table S1; [10]). In addition to performing simulations with the maximum dissolved phosphate concentrations measured in the Great Lakes (i.e., 15 µg L^{−1} in Western Lake Erie; [42]), additional simulations were performed with phosphate solution levels that were adjusted to phosphate targets set by the Great Lakes Water Quality Agreement (GLWQA; International Joint Commission (IJC); Table S2; [42,43]), which ranged between 5 and 15 µg L^{−1} for the upper Great Lakes versus Western Lake Erie, respectively.

All other solution variables were kept constant in the above simulations, according to a one-at-a-time sensitivity analysis, where the solution charge balance was used as a model performance indicator, as described above.

3. Results and Discussion

3.1. General Solution Chemistries and Model Charge Balance

Surface water compositions of the Great Lakes connecting channels were representative of their long-term freshwater chemistries [3], with alkalinity ranging only slightly between 41 and 133 mg L⁻¹, the sum of Ca and Mg concentrations varying between 15 and 50 mg L⁻¹ and those of Cl and SO₄ varying more strongly, from <2 to >25 mg L⁻¹, upstream-to-downstream across the basin (Table S1). The overall hydrogeochemical compositions suggest waters of the calcium/magnesium bicarbonate-type, albeit with increasing salinification upstream-to-downstream, as indicated in Figure 1. The pH of the connecting channel waters gradually increased from 7.2 ± 0.1 to 7.5 ± 0.1 (~40% decrease in proton activity), inversely correlated to carbonate alkalinity (15% increase) and the oxidation-reduction potential ranged from 393 ± 43 to 315 ± 70 mV (decreasing upstream-to-downstream), reflective of well-oxygenated, reasonably circumneutral freshwaters.

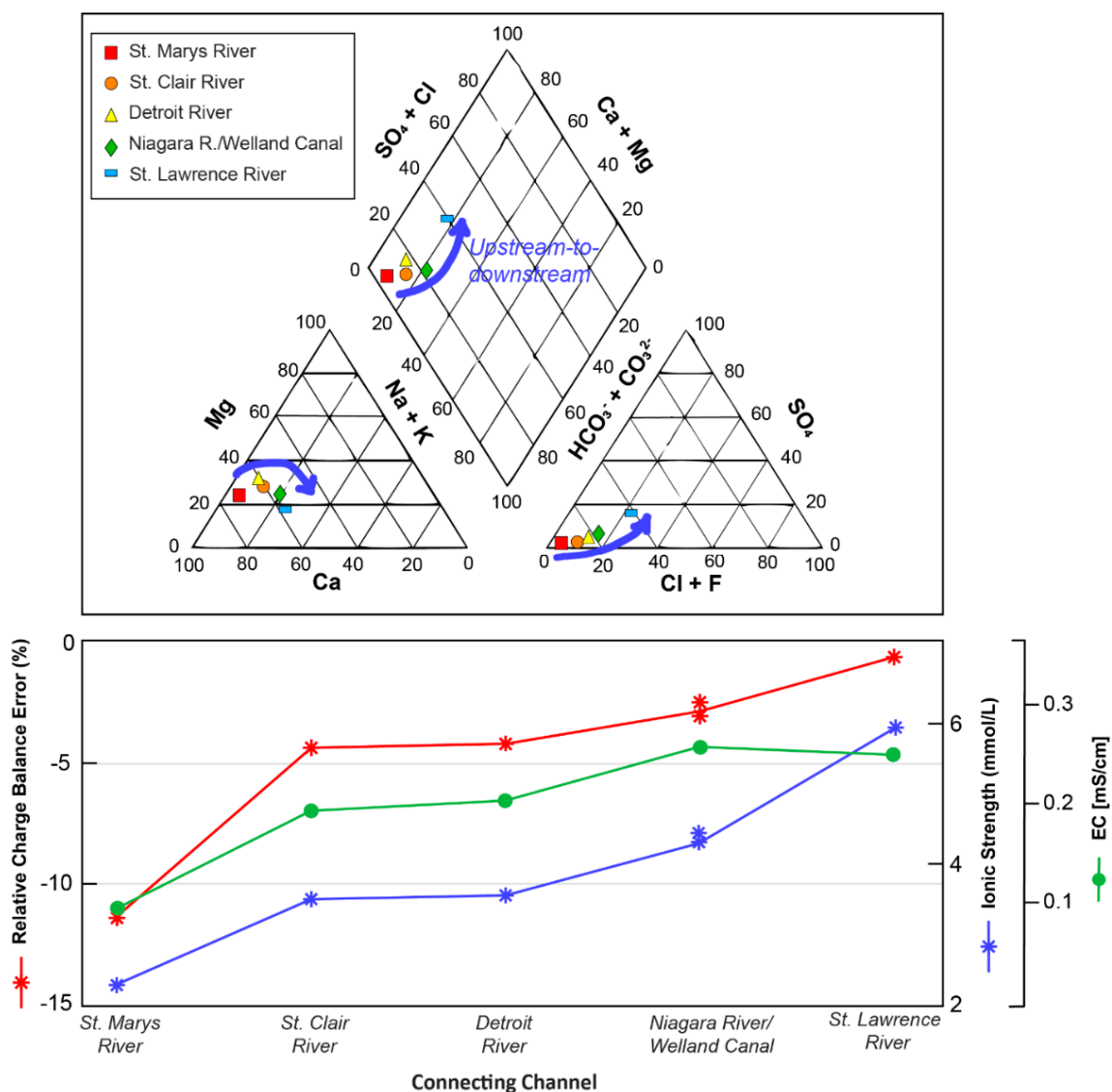


Figure 1. Top frame: major ion geochemistry of the connecting channel surface waters in a Piper Ternary diagram (%-meq L⁻¹ for all axes), and, bottom frame: comparison of simulated charge balance (% error; left y-axis) to ionic strength and electric conductivity (right y-axes) across the simulated connecting channel surface waters.

The simulated chemical compositions of connecting channel waters (Table S1) yielded relative charge balance errors of up to -12% , indicating excess net-negative charges in solution, particularly in the northernmost connecting channel, the St. Marys River (Figure 1). The charge imbalance decreased in the relative magnitude upstream-to-downstream and was $<5\%$ for all other channels. The residual relative charge imbalance reduces with increasing ionic strength and conductivity of the waters (Figure 1), suggesting a gradual over-imprinting of the aqueous electron imbalance with increasing salinification upstream-to-downstream. Probable causes underlying the observed charge imbalances include changes in pH and redox state within and between the averaged individual locations, or analytical uncertainty, i.e., underestimated cation concentrations, overestimated anion concentrations, or a combination of the above. For example, modulation of the pH predicted an increase of -0.1 pH units to achieve charge parity, which is within the uncertainty for the deployed field probes. Alternatively, variation of the aqueous Ca concentration, the most abundant doubly charged cation, predicted an increase in the simulated Ca molality of $\sim 120\%$, which is within the range of variability of total Ca concentrations in connecting channel waters [6], yet above the analytical uncertainty for this parameter. Finally, even though additional charged ions or solutes (nitrogen compounds, halogens other than Cl) as well as suspended particulates if present, may have contributed to the residual charge imbalance, the obtained agreements suggest that the considered suite of aqueous parameters captures the general composition of the modeled surface waters.

3.2. Trends in Aqueous Trace Element Speciation across the Great Lakes

The simulated aqueous speciation of the studied major and trace elements in the studied waters suggests that for most elements, a single oxidation state was typically dominant by several orders of magnitude, including for redox-sensitive elements (e.g., As, Cu, V). Resulting from the relatively narrow range of simulated redox conditions (see p_e in Table S1), this corroborated previous data on select redox couples measured in these Great Lakes connecting channel samples, i.e., the majority of total S being present as sulphate and no detectable Fe[+2] (at least 1000-times less abundant than Fe[+3]) [10,44]. Yet, there were select trace elements where more than one oxidation state was relevant to the overall aqueous species distribution, including Cr[+3] versus Cr[+6] or Se[+4] versus Se[+6] (see below).

The following discussion focuses on eight of the investigated trace elements: the alkaline earth metals Li and Rb, the transition metals Mn and Ni, the oxyanion-forming transition metal V and non-metal Se, and the rare earth elements Ce and Gd. The aqueous speciation of these trace elements appeared to be dominated by inorganic species (i.e., non-DOM-bound), namely monovalent cations for Li and Rb, oxyanionic species for V and Se, and carbonate and phosphate complexes for Ce and Gd (Figure 2), although aqueous complexes with Cl and SO_4 were also present for other trace elements. Only the aqueous species at $>0.01\%$ abundance within each of the trace element distributions are discussed below; other species present at lower abundance were considered unlikely to exert significant control on trace element dynamics in the areas of interest. Overall, the aqueous speciation of trace elements did not vary significantly between species upstream-to-downstream, even though some of their absolute concentrations and that of ligating ions such as Cl and SO_4 varied considerably (Table S1).

The dominance of monovalent alkali metal cations at $>99.9\%$ remained virtually constant across the basin, including for trace elements such as Li and Rb (Figure 2). Aqueous alkali metal complexes with sulfate and chloride as ligands occurred for the most downstream connecting channel (St. Lawrence) but only at relative abundances $<0.03\%$. The aqueous speciation of the alkali trace metals Li and Rb thus appears to be similar to that of Na and K, existing predominantly as monovalent cations that only weakly interact with suspended mineral or organic matter [45–47] and may therefore be assumed to behave reasonably conservative in oxic surface waters, compared to the other trace elements discussed below [10].

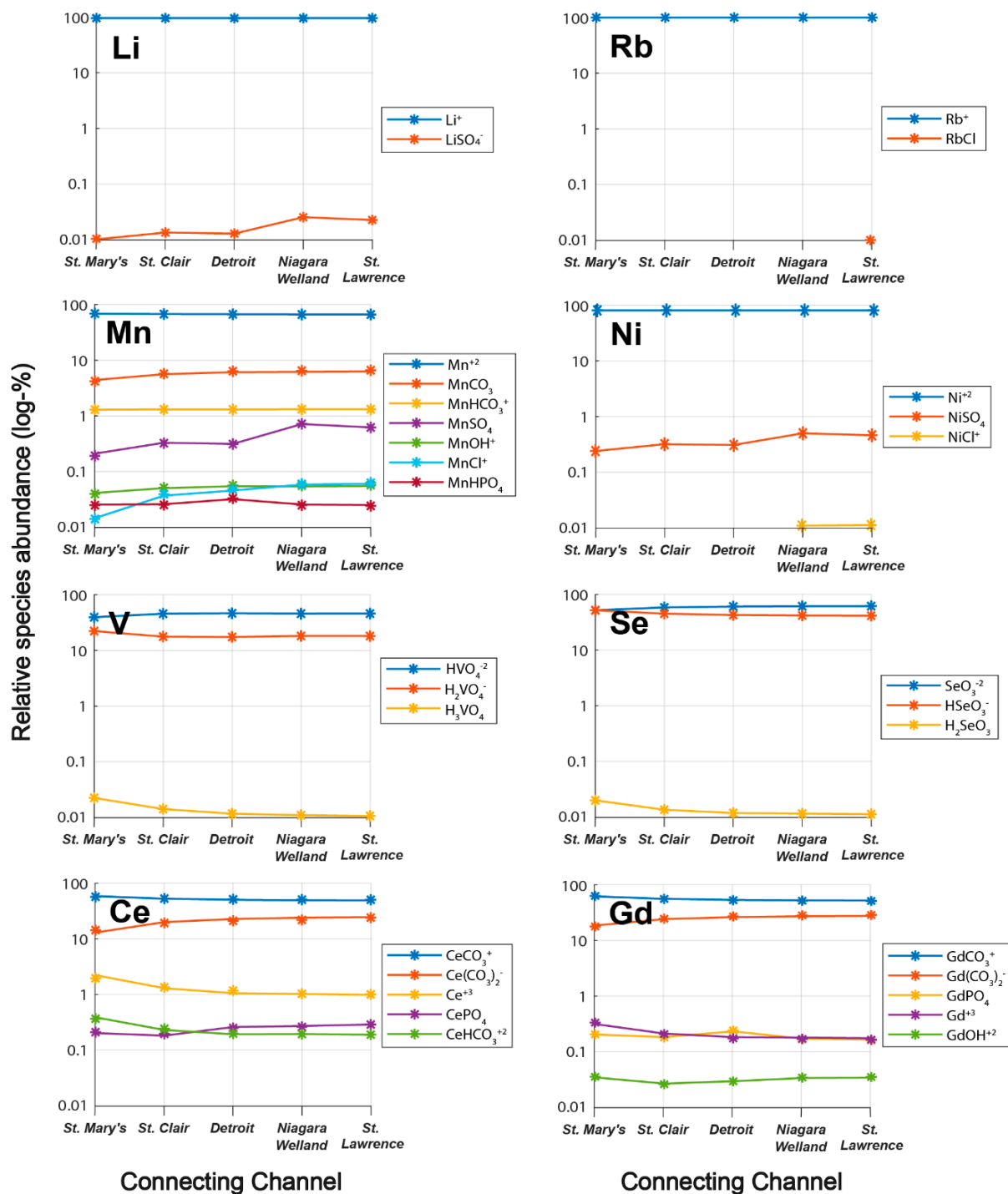


Figure 2. Geochemical equilibrium modelling of the aqueous speciation of select trace elements in the connecting channels of the Great Lakes basin. Plotted is the share of major individual aqueous species per-total (molality basis), upstream-to-downstream for the connecting channels; additional species present at a <0.01% share are not shown.

In contrast to the uniform speciation of Li and Rb, the transition elements Mn and Ni speciated more diversely in the solution (Figure 2). While divalent cations were the dominant aqueous species for both elements in all connecting channels at >90% relative abundance, Ni also tended to speciate with sulfate complexes and Mn was distributed among carbonate, hydrate, sulfate, chloride, and phosphate species, all at abundances >0.03%. The relative importance of the complexed Mn and Ni species over their free

cationic species increased upstream-to-downstream in the connecting channel samples, likely the result of the increasing ligand concentrations further downstream in the basin (Table S1). Overall, while the total concentrations of dissolved Mn and Ni between the connecting channels changed with a factor of nine and five, respectively, the dissolved fraction remained consistently dominated by divalent cations at >1 order of magnitude excess over the next abundant species.

The oxyanion-forming elements V and Se displayed a consistent distribution, existing as oxyanionic species with charges that varied with up to ~35% across the connecting channels and no other ligands predicted at >0.01% relative abundance (Figure 2). In contrast to the previously discussed trace elements, the most abundant V and Se oxyanions were less dominant than other species. For instance, the relative abundance of the two most abundant species of Se[+4], $\text{SeO}_3[-2]$ and $\text{HSeO}_3[-1]$, was close to ~50%, each (Figure 2), explained by the fact that the pH of the connecting channel waters was very close to the first protonation constant pK_{a1} of Se[+4] (7.28 in the LLNL database). Similarly, the pK_{a2} for $\text{HVO}_4[-1]$ is 7.09. Both dissolved V and Se species may thus be expected to deprotonate as a result of slightly increasing pH upstream-to-downstream across the basin, and these double-negatively charged oxyanions to gain prominence of single-negatively charged oxyanions. Such increases in the share of negatively charged V and Se anions will impact their propensity to adsorb to suspended particles in the water column and could be investigated in future research.

Finally, the geochemical simulations suggest aqueous complexation of the rare earth elements (REE) Ce and Gd with carbonate (>99%) and, to a lesser extent, phosphate (<0.5%). Carbonate and phosphate ions are typically the dominant inorganic ligands involved in freshwater REE complexation [48]. In the connecting channels, carbonate complexation dominates over phosphate in the percent share of species, as well as the preferential complexation by carbonates over bicarbonates at pH range of 7–8: extensive phosphate-complexation is not expected due to the high $[\text{HCO}_3^-]/[\text{HPO}_4^{2-}]$ ratio and circumneutral pH, as well as relatively high Ca and Mg abundance in the Great Lakes [48,49]. As such, the relatively consistent Ce and Gd speciations across the basin are likely the result of ditto general water quality (i.e., pH, alkalinity, and phosphate) upstream-to-downstream.

Overall, the simulated trace element speciation in the Great Lakes connecting channels appeared spatially similar, in line with reasonably consistent elemental concentrations and pHs (Table S1). In addition, variations in other major quality parameters, such as the potential ligands DOM, Cl, SO_4 , and alkalinity (Figure 2) appeared insufficient to affect trace element speciation significantly.

3.3. Stable Trace Element Speciation with Changing Great Lakes Water Quality

In addition to examining spatial patterns, geochemical equilibrium simulations were used to investigate the potential changes to aqueous trace element speciation under imposed changing water quality (see Section 2.3). Below, we discuss select elements from the trace elements discussed above in the various examined scenarios.

3.3.1. Temperature

Future changes to summer surface water temperatures in the Great Lakes are difficult to ascertain because of regional differences in climate and circulation dynamics, but depending on the climate projection chosen, have been estimated to range from roughly 1.5 to 6.5 degrees [50,51]. While other seasons may be several degrees cooler than the measured summer surface temperature, system sensitivity was assessed using a range of $\pm 10^\circ\text{C}$ up to 2100 (Table S2).

The equilibrium modelling simulations show that V and Se were among the elements that displayed the most pronounced changes in speciation with increasing temperatures across the investigated trace elements. In the most upstream investigated connecting channel, the St. Mary's River, the relative abundances of monovalent $\text{HSeO}_3[-1]$ and $\text{H}_2\text{VO}_4[-1]$ are simulated to decrease by 6% and 10%, respectively, upon increasing temper-

ature, while their divalent counterparts, $\text{SeO}_3[-2]$ and $\text{HVO}_4[-2]$, are simulated to increase by 7.6% and 4.1%, respectively (Figure 3). In the most downstream investigated connecting channel (St. Lawrence River), the relative abundances of monovalent $\text{HSeO}_3[-1]$ and $\text{H}_2\text{VO}_4[-1]$ are similarly simulated to decrease by 7% and 12%, respectively, with higher water temperatures, while their divalent counterparts, $\text{SeO}_3[-2]$ and $\text{HVO}_4[-2]$, increase by 5.4% and 3.1%, respectively (Figure 3). For the investigated scenarios and solutions, the decrease in the charge balance agreement (-0.05%) was negligible (data not shown). The extrapolated conditions thus reveal that, with higher water temperatures, the prevalence of divalent V and Se oxyanions increases and thereby increases the net-negative charge on these oxyanionic trace element species.

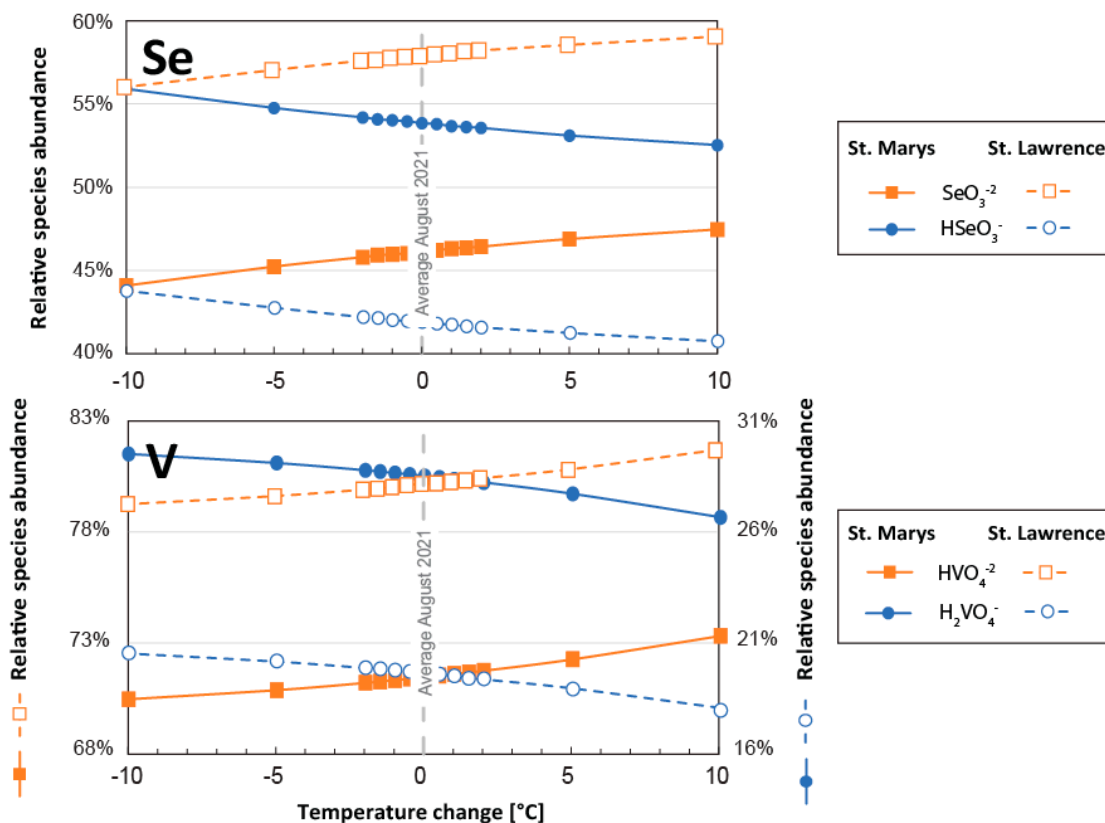


Figure 3. Geochemical equilibrium modelling of the aqueous speciation of Se (top frame) and V (bottom frame) in the St. Marys and St. Lawrence rivers in the Great Lakes basin. Plotted is the share of select individual aqueous species per elemental-total (molality basis, note the two y-axes for bottom frame) as a function of temperature.

The temperature dependence of the reaction equilibrium constants K in PHREEQC is calculated using Van ‘t Hoff’s equation that may be expressed as:

$$\ln \frac{K_2}{K_1} = \frac{\Delta H^\circ}{R} - \left(\frac{1}{T_1} - \frac{1}{T_2} \right) \tag{1}$$

where ΔH is the standard reaction enthalpy, T is temperature and R is the ideal gas constant. According to the LLNL database, the enthalpy of reaction for the deprotonation of selenite ($\text{HSeO}_3^- \rightleftharpoons \text{SeO}_3^{2-} + \text{H}^+$) is 5.35 kJ/mol, from which it follows that the equilibrium constant for this reaction increases by a factor of 1.9 at the investigated 10 °C temperature increase. This factor exceeds the simulated by a <10% difference in individual species abundance discussed above, which is explained by temperature changes inducing the re-distribution of all considered equilibrium constants and charge solutes in solution. This demonstrates that while the simulated changes in trace element speciation as a function of

temperature appear relatively minor, an understanding of temperature-induced shifts in solute speciation thus requires consideration of the full solution chemistry.

3.3.2. Salinity

Changes to salinity levels were extrapolated from previous assessments of the long-term trends of chloride concentrations in the Great Lakes by adopting linearized rates of change for each lake and, therefore, its preceding connecting channels [41]. Total dissolved chloride concentrations forecasted for 2050 and 2100 are expected to increase by up to $180 \mu\text{g L}^{-1}$ (St. Marys River, 2050) to $>12,000 \mu\text{g L}^{-1}$ (East Lake Erie/Niagara River, 2100 projection; Table S2) relative to 2021 data, stemming from Lakes Erie and Ontario being subjected to more rapid rates of salinification.

As expected, the geochemical equilibrium simulations reveal that Cl remains present in the free monovalent anionic form ($\text{Cl}[-1]$), at up to 4 orders of magnitude above the next most abundant Cl-species, among the entire investigated salinity range (data not shown). Chloride that was added to the higher-salinity scenarios mostly speciated to major elements such as Ca ($\text{CaCl}[+1]$), Mg ($\text{MgCl}[+1]$), Na (NaCl), K (KCl) and Sr ($\text{SrCl}[+1]$), in line with the elemental abundance of these ions in the connecting channel waters. Consequently, only minor amounts of the introduced Cl ligated to scarcer trace elements, with shifts in the relative abundance of Cl-complexes within individual elemental speciation patterns in accordance with the imposed change in salinity. For instance, the relative abundance of Cl-complexes increased for Li, Mn, and Zn at rates of $\sim 21\%$ for the St. Mary's River and $\sim 71\%$ for the St. Lawrence River at increasing salinities, albeit at low overall relative abundance ($<0.1\%$) (Figure 4). These increases match to within a percent of the simulated increases in salinity for these connecting channels (21% and 72%, respectively; Table S2). For Ca, the relative abundance of Cl complexes slightly decreased at the highest simulated salinity scenario (Figure 4), potentially due to out-competing the other cations (Mg, Na, present at similar concentrations ranges), or the reduced solubility of carbon dioxide and Ca-carbonates due to increasing ionic strengths. The observed changes in the trace element speciation as a function of salinity (chloride exclusively) thus appear relatively minor, but further work is required to disentangle the potential influence of concurrent changes in other solutes that will affect the solution chemistry (Na or SO_4 ; [3]).

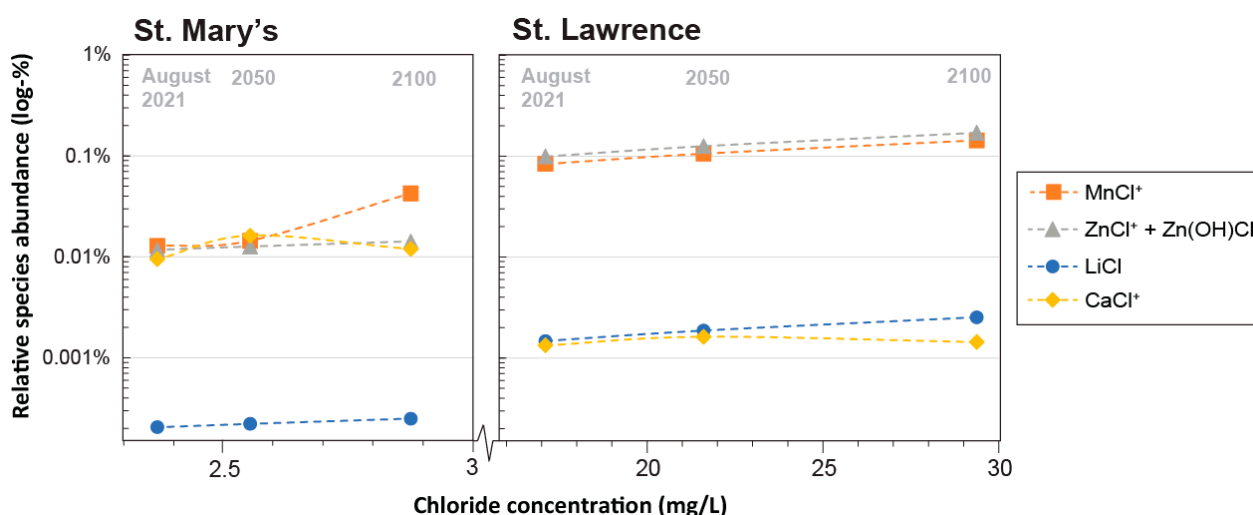


Figure 4. Geochemical equilibrium modelling of the relative abundance of select aqueous Cl-complexes of Mn, Zn, Li and Ca in the St. Marys (upstream, left panel) and St. Lawrence (downstream, right panel) rivers in the Great Lakes basin. Plotted is the share of select individual aqueous species per-total (molality basis, logarithmic y-axis) as a function of Cl concentration (intersected x-axis).

3.3.3. Alkalinity

Like the performed simulations of increased salinity, simulated scenarios with alkalinity variations in the Great Lakes were derived from linearized trends adopted from long-term field observations [3]. Dissolved carbonate concentrations are therefore predicted to increase between 2050 and 2100, with larger rates of change observed for the lower lakes (e.g., from $580 \mu\text{g L}^{-1}$ in the St. Mary's River by 2050 to $>11,000 \mu\text{g L}^{-1}$ in East Lake Erie and the Niagara River by 2100; Table S2).

The simulated increases in alkalinity ranged from +4% in the St. Mary's River to +13% in the Lawrence River and induced negligible changes in the relative abundance of dissolved HCO_3^- and CO_3^{2-} throughout the basin (pH dependence of the carbonate equilibrium between pH 7.2–7.5). Further, higher alkalinity increased the proportion of the carbonate-complexed Ca and Mg, as well as that of Cu, Zn, Mn, and Fe-carbonates, but to different extents throughout the basin. For instance, the projected relative abundance of Mn-carbonates increased by only $<0.1\%$ in the St. Mary's River but by $>1\%$ in the St. Lawrence River (Figure 5). Generally, the aqueous speciation of REEs was observed to move from mono- to di-carbonated complexes (REE-CO_3 versus $\text{REE-(CO}_3)_2$), e.g., as observed with $\sim 5\%$ and $\sim 1\%$ increases in doubly complexed Ce and Gd in the St. Lawrence and St. Mary's, respectively. However, total net increases in carbonate-complexed Ce and Gd species were low ($<1\%$) because these elements were strongly ligated by carbonates initially (i.e., compared to the larger total change in Mn-carbonate complexation). Although shifts in aqueous trace element speciation were observed to be minor overall, the relative effects of increased alkalinity may be more pronounced in the upper lakes where alkalinity is lower [10] and warrant further investigation of the consequences, e.g., carbonate precipitation and adsorption.

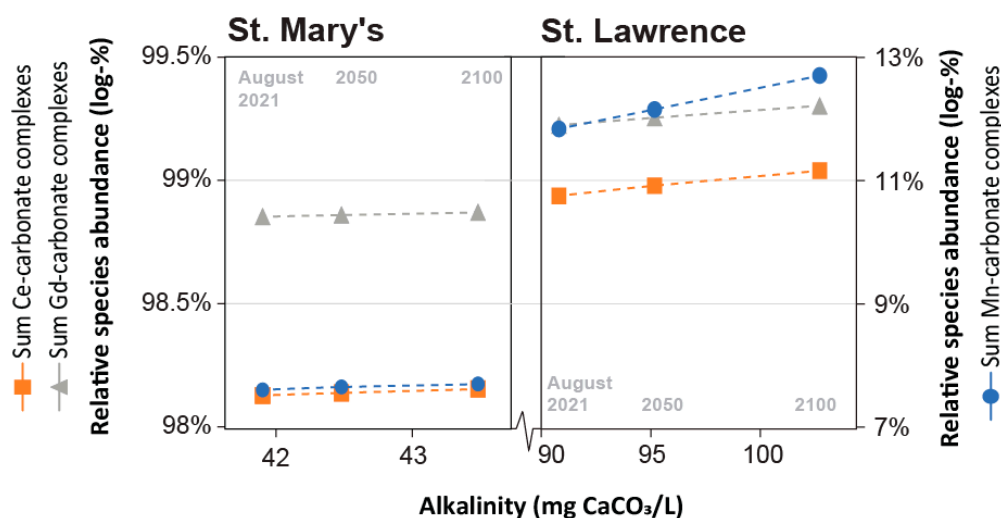


Figure 5. Geochemical equilibrium modelling of the relative abundance of aqueous carbonate complexes of Ce and Gd (left y-axis) and Mn (right y-axis) in the St. Mary's (upstream, left panel) and St. Lawrence (downstream, right panel) rivers in the Great Lakes basin. Plotted is the combined share of all carbonate-complexed aqueous species per-total (molality basis) as a function of alkalinity (intersected x-axis).

3.3.4. Phosphate

Previous work has revealed gradually decreasing P concentrations in the Great Lakes' surface waters [41]. As extrapolation of such P rates to 2050 and 2100 would effectively yield zero dissolved phosphorus, a minimum boundary of phosphate was established from the GLWQA concentration targets established for the Great Lakes [19,43]. Comparisons are thus drawn between the current (2021) baseline state and targeted long-term average concentrations.

Phosphorus speciated mostly as free anionic $\text{HPO}_4[-2]$ and $\text{H}_2\text{PO}_4[-1]$, followed by monovalent and divalent Ca and Mg complexes, respectively. Phosphate complexes with Na, Zn, K, Sr, and Mn were also simulated, and, in line with their lower abundance, phosphate complexes with other trace elements as well (e.g., REE-phosphates at log activities below 10^{-11}). Despite their low abundance, the activities of phosphate-complexed trace elements did change as a function of the dissolved phosphate concentration (see examples of REE in Figure 6). For instance, the singly phosphate-ligated REE- $\text{PO}_4[0]$ complexes were over an order of magnitude more abundant than the REE- $\text{HPO}_4[+1]$, REE- $(\text{PO}_4)_2[-3]$, REE- $(\text{H}_2\text{PO}_4)[+2]$, and REE- $\text{HPO}_4[-1]$ species under all simulated phosphate levels, yet they became more important at lower PO_4 -concentrations target by the GLWQA, at the expense of positively charged REE- PO_4 complexes. Overall, decreasing phosphate levels led to a lower complexation of REE and therefore less negatively (or more positively) phosphate-bound REE fraction, as well as a lesser extent of PO_4 -ligated REE overall (Figure 6). Because the relative abundance of PO_4 -complexed REE is small relative to that of carbonate-ligated REE, the effect of reducing PO_4 levels on the REE cycling may be expected to be minor. However, given the heterogeneous occurrence of the dissolved PO_4 levels in the Great Lakes as a result of point- and non-point-sourced phosphate inputs and scavenging in the water column [19,52], the impact of such fluctuations on trace element dynamics, especially for elements such as the REE that display highly erratic spatial concentration patterns [10], warrants further investigation.

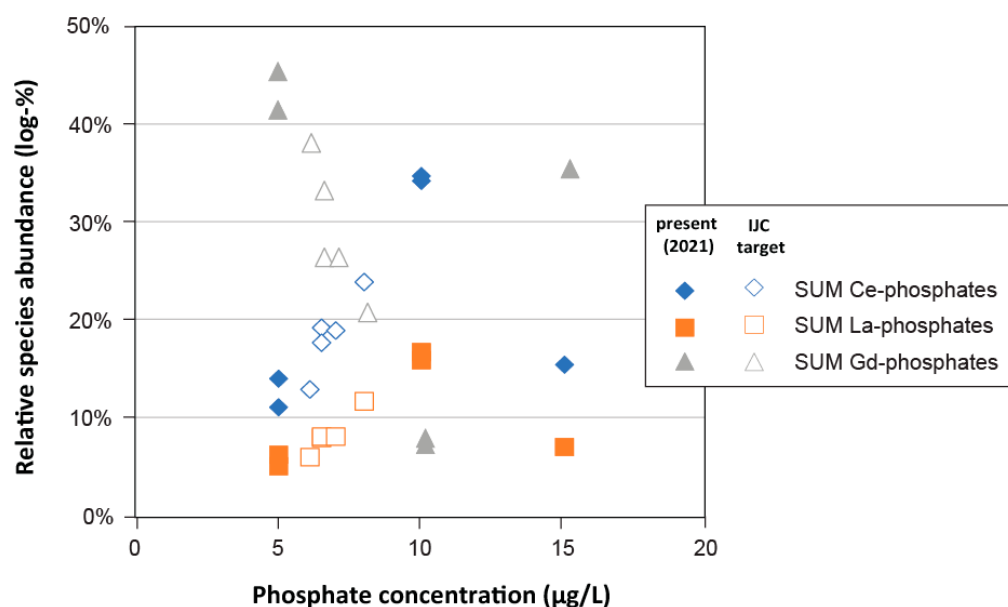


Figure 6. Geochemical equilibrium modelling of the relative abundance of aqueous phosphate complexes of La, Ce and Gd in the various connecting channels in the Great Lakes basin. Plotted is the share of aqueous rare earth element phosphate species per-total (molality basis) as a function of the phosphate concentration (present versus IJC targets; x-axis).

4. Conclusions

This study provided insights into the aqueous speciation of select trace elements in Great Lakes connecting channel water samples. From geochemical equilibrium modelling of averaged solute concentrations across surface water sampling locations throughout the basin, we conclude that:

- The aqueous speciation of most trace elements appears relatively consistent across the basin, in line with a comparatively stable water quality (pH, alkalinity) upstream-to-downstream across the Great Lakes. Trace element complexation with ligands such as phosphate or chloride generally followed basin-wide trends in salinity or nutrient levels;

- Alkali trace metals (Li, Rb) are dominantly speciated as free monovalent cations, oxyanion-forming elements (Se, V) as oxoacids, rare earth elements (La, Ce, Gd) as carbonates, and various other trace elements as complexes with sulfate or phosphate;
- Simulations of aqueous trace element speciation under extrapolated future water quality scenarios (e.g., increased temperature, salinity, varying alkalinity, and phosphate) suggest that the speciation of most trace elements is robust, not only spatially, but temporally as well.

Our analysis was conducted with emphasis on the inorganic aqueous speciation, preventing us from assessing the biogeochemical fate of trace elements in the water column (e.g., partitioning of dissolved trace elements to suspended solids and sedimentation) or biological effects and feedbacks induced by changing nutrient levels, the increasing osmotic pressure from salinification, or the bioavailability of essential micronutrient trace elements. The inclusion of additional water quality data (nitrogen, organic matter) in geochemical equilibrium and kinetic modelling may be used when considering the above processes. Further monitoring of trace element dynamics in the Great Lakes is generally required to improve such models and to examine the role of speciation in trace element dynamics in other waters in the Great Lakes basin (e.g., in tributaries or at the nearshore-offshore interface). A refined understanding of the behaviours and fates of trace elements in the Great Lakes will help water quality managers predict and manage potential changes in this complex freshwater system.

Supplementary Materials: The following supporting information can be downloaded at: <https://www.mdpi.com/article/10.3390/w15081483/s1>, Table S1: Connecting channel hydrochemistry used in simulations; Table S2. Extrapolated parameters used in simulations (based on 2021 data).

Author Contributions: Conceptualization, J.F.; methodology, J.F. and C.B.; validation and formal analysis; J.F. and B.V.; writing—original draft preparation, J.F.; writing—review and editing, C.B. and B.V. All authors have read and agreed to the published version of the manuscript.

Funding: This research was funded by the Natural Sciences and Engineering Research Council (NSERC), Canada, grant number 2021-03133.

Data Availability Statement: All data used in this study are available in the Supplementary Material.

Conflicts of Interest: The authors declare no conflict of interest.

References

1. Behmel, S.; Damour, M.; Ludwig, R.; Rodriguez, M.J. Water quality monitoring strategies—A review and future perspectives. *Sci. Total Environ.* **2016**, *571*, 1312–1329. [[CrossRef](#)] [[PubMed](#)]
2. Mahdiyan, O.; Filazzola, A.; Molot, L.A.; Gray, D.; Sharma, S. Drivers of water quality changes within the Laurentian Great Lakes region over the past 40 years. *Limnol. Oceanogr.* **2020**, *66*, 237–254. [[CrossRef](#)]
3. Chapra, S.C.; Dove, A.; Warren, G.J. Long-term trends of Great Lakes major ion chemistry. *J. Great Lakes Res.* **2012**, *38*, 550–560. [[CrossRef](#)]
4. Sterner, R.W.; Ostrom, P.; Ostrom, N.E.; Klump, J.V.; Steinman, A.D.; Dreelin, E.A.; Zanden, M.J.V.; Fisk, A.T. Grand challenges for research in the Laurentian Great Lakes. *Limnol. Oceanogr.* **2017**, *62*, 2510–2523. [[CrossRef](#)]
5. Hartig, J.H.; Krantzberg, G.; Alsip, P. Thirty-five years of restoring Great Lakes Areas of Concern: Gradual progress, hopeful future. *J. Great Lakes Res.* **2020**, *46*, 429–442. [[CrossRef](#)]
6. Hill, B.; Dove, A. Concentrations and loads of nutrients and major ions in the Niagara River, 1975–2018. *J. Great Lakes Res.* **2021**, *47*, 844–861. [[CrossRef](#)]
7. Elliott, S.M.; Brigham, M.E.; Lee, K.E.; Banda, J.A.; Choy, S.J.; Gefell, D.J.; Minarik, T.A.; Moore, J.N.; Jorgenson, Z.G. Contaminants of emerging concern in tributaries to the Laurentian Great Lakes: I. Patterns of occurrence. *PLoS ONE* **2017**, *12*, e0182868. [[CrossRef](#)]
8. Sterner, R.W. The Laurentian Great Lakes: A Biogeochemical Test Bed. *Annu. Rev. Earth Planet. Sci.* **2021**, *49*, 201–229. [[CrossRef](#)]
9. Ozersky, T.; Bramburger, A.J.; Elgin, A.K.; Vanderploeg, H.A.; Wang, J.; Austin, J.A.; Carrick, H.J.; Chavarie, L.; Depew, D.C.; Fisk, A.T.; et al. The changing face of winter: Lessons and questions from the Laurentian great lakes. *J. Geophys. Res. Biogeosci.* **2021**, *126*, e2021JG006247. [[CrossRef](#)]
10. Bentley, C.; Fitzgerald, Dove, A.; Richardson, V.; Bradley, L.; Vriens, B. Trace Element Loads in the Great Lakes Basin: A Reconnaissance. *J. Great Lakes Res.* **2023**; *in press*. [[CrossRef](#)]

11. Baehr, M.M.; McManus, J. The measurement of phosphorus and its spatial and temporal variability in the western arm of Lake Superior. *J. Great Lakes Res.* **2003**, *29*, 479–487. [[CrossRef](#)]
12. Chen, C.; Kamman, N.; Williams, J.; Bugge, D.; Taylor, V.; Jackson, B.; Miller, E. Spatial and temporal variation in mercury bioaccumulation by zooplankton in Lake Champlain (North America). *Environ. Pollut.* **2012**, *161*, 343–349. [[CrossRef](#)]
13. Coale, K.H.; Flegal, A.R. Copper, zinc, cadmium and lead in surface waters of Lakes Erie and Ontario. *Sci. Total Environ.* **1989**, *87–88*, 297–304. [[CrossRef](#)]
14. Rossman, R.; Barres, J. Trace Element Concentrations in Near-Surface Waters of the Great Lakes and Methods of Collection, Storage, and Analysis. *J. Great Lakes Res.* **1988**, *14*, 188–204. [[CrossRef](#)]
15. Nriagu, J.O.; Lawson, G.; Wong, H.K.T.; Cheam, V. Dissolved Trace Metals in Lakes Superior, Erie, and Ontario. *Environ. Sci. Technol.* **1995**, *30*, 178–187. [[CrossRef](#)]
16. Yuan, F.; Chaffin, J.; Xue, B.; Wattus, N.; Zhu, Y.; Sun, Y. Contrasting sources and mobility of trace metals in recent sediments of western Lake Erie. *J. Great Lakes Res.* **2018**, *44*, 1026–1034. [[CrossRef](#)]
17. Aliff, M.N.; Reavie, E.D.; Post, S.P.; Zanko, L.M. Metallic elements and oxides and their relevance to Laurentian Great Lakes geochemistry. *PeerJ* **2020**, *8*, e9053. [[CrossRef](#)]
18. Bentley, C.; Junqueira, T.; Dove, A.; Vriens, B. Mass-balance Modeling of Metal Loading Rates in the Great Lakes. *Environ. Res.* **2022**, *205*, 112557. [[CrossRef](#)]
19. Dove, A.; Chapra, S.C. Long-term trends of nutrients and trophic response variables for the Great Lakes: Great Lakes nutrient trends. *Limnol. Oceanogr.* **2015**, *60*, 696–721. [[CrossRef](#)]
20. Bazzi, A.; Lehman, J.T.; Nriagu, J.O.; Hollandsworth, D.; Irish, N.; Noshier, T. Chemical Speciation of Dissolved Copper in Saginaw Bay, Lake Huron, with Square Wave Anodic Stripping Voltammetry. *J. Great Lakes Res.* **2002**, *28*, 466–478. [[CrossRef](#)]
21. Twiss, M.R.; Campbell, P.G.C. Scavenging of ¹³⁷Cs, ¹⁰⁹Cd, ⁶⁵Zn, and ¹⁵³Gd by plankton of the microbial food web in pelagic Lake Erie surface waters. *J. Great Lakes Res.* **1998**, *24*, 776–790. [[CrossRef](#)]
22. Twiss, M.R.; Campbell, P.G.C. Trace metal cycling in the surface waters of Lake Erie: Linking ecological and geochemical fates. *J. Great Lakes Res.* **1998**, *24*, 791–807. [[CrossRef](#)]
23. Leal, A.M.M.; Kulik, D.A.; Smith, W.R.; Saar, M.O. An overview of computational methods for chemical equilibrium and kinetic calculations for geochemical and reactive transport modeling. *Pure Appl. Chem.* **2017**, *89*, 597–643. [[CrossRef](#)]
24. Seigneur, N.; Mayer, K.U.; Steefel, C.I. Reactive transport in evolving porous media. *Rev. Mineral. Geochem.* **2019**, *85*, 197–238. [[CrossRef](#)]
25. Caruso, B.S.; Cox, T.J.; Runkel, R.L.; Velleux, M.L.; Bencala, K.E.; Nordstrom, D.K.; Julien, P.Y.; Butler, B.; Alpers, C.; Marion, A.; et al. Metals fate and transport modelling in streams and watersheds: State of the science and USEPA workshop review. *Hydrol. Process.* **2008**, *22*, 4011–4021. [[CrossRef](#)]
26. Schecher, W.D.; McAvoy, D.C. MINEQL+, A Software Environment for Chemical Equilibrium Modeling. *Comput. Environ. Urban Syst.* **1992**, *16*, 65–76. [[CrossRef](#)]
27. Parkhurst, D.L. *User's Guide to PHREEQC, a Computer Model for Speciation, Reaction-Path, Advective-Transport and Inverse Geochemical Calculations*; US Geological Survey Water-Resources Investigations Report 95-4227; U.S. Geological Survey: Reston, VA, USA, 1995.
28. Haase, C.; Ebert, M.; Dethlefsen, F. Uncertainties of geochemical codes and thermodynamic databases for predicting the impact of carbon dioxide on geologic formations. *Appl. Geochem.* **2016**, *67*, 81–92. [[CrossRef](#)]
29. Zhu, C.; Nordstrom, D.K. Flying Blind: Geochemical Modeling and Thermodynamic Data Files. *Groundwater* **2022**, *60*, 699–700. [[CrossRef](#)]
30. Mühr-Ebert, E.L.; Wagner, F.; Walther, C. Speciation of uranium: Compilation of a thermodynamic database and its experimental evaluation using different analytical techniques. *Appl. Geochem.* **2019**, *100*, 213–222. [[CrossRef](#)]
31. Ball, J.W.; Nordstrom, D.K. *User's Manual for WATEQ4F, with Revised Thermodynamic Database and Test Cases for Calculating Speciation of Major, Trace, and Redox Elements in Natural Waters*; US Geological Survey Open File Report 91-183; U.S. Geological Survey: Reston, VA, USA, 1991.
32. Zhu, C.; Anderson, G. *Environmental Applications of Geochemical Modeling*; Cambridge University Press: Cambridge, UK, 2002.
33. Quinn, F.H. Hydraulic residence times for the Laurentian great lakes. *J. Great Lakes Res.* **1992**, *18*, 22–28. [[CrossRef](#)]
34. EGLE, State of Michigan, Department of the Environment, Great Lakes and Energy. Great Lakes Connecting Channel—Water Quality Data, 2020 Integrated Report. 2020. Available online: <https://www.michigan.gov/-/media/Project/Websites/egle/Documents/Programs/WRD/SWAS/ir2020-all.pdf?rev=2983e2380a7a438a86a0d636077ceb51> (accessed on 1 October 2022).
35. Smith, R.E.H.; Allen, C.D.; Charlton, M.N. Dissolved Organic Matter and Ultraviolet Radiation Penetration in the Laurentian Great Lakes and Tributary Waters. *J. Great Lakes Res.* **2004**, *30*, 367–380. [[CrossRef](#)]
36. Zhou, Z.; Guo, L.; Minor, E.C. Characterization of bulk and chromophoric dissolved organic matter in the Laurentian Great Lakes during summer 2013. *J. Great Lakes Res.* **2016**, *42*, 789–801. [[CrossRef](#)]
37. Allison, J.D.; Brown, D.S.; Novo-Gradac, K.J. *MINTEQA2/PRODEFA2—A Geochemical Assessment Model for Environmental Systems. Version 3.0 User's Manual*; Environmental Research Laboratory, Office of Research and Development U.S. Environmental Protection Agency: Athens, GA, USA, 1998.
38. Blanc, P.; Lassin, A.; Piantone, P.; Azaroual, M.; Jacquemet, N.; Fabbri, A.; Gaucher, E. Thermoddem: A geochemical database focused on low temperature water/rock interactions and waste materials. *Appl. Geochem.* **2012**, *27*, 2107–2116. [[CrossRef](#)]

39. Trumpickas, J.; Shuter, B.J.; Minns, C.K. Forecasting impacts of climate change on Great Lakes surface water temperatures. *J. Great Lakes Res.* **2009**, *35*, 454–463. [[CrossRef](#)]
40. Dugan, H.A.; Bartlett, S.L.; Burke, S.M.; Doubek, J.P.; Krivak-Tetley, F.E.; Skaff, N.K.; Summers, J.C.; Farrell, K.J.; McCullough, I.M.; Morales-Williams, A.M.; et al. Salting our freshwater lakes. *Proc. Natl. Acad. Sci. USA* **2017**, *114*, 4453–4458. [[CrossRef](#)]
41. Chapra, S.C.; Dove, A.; Rockwell, D.C. Great Lakes chloride trends: Long-term mass balance and loading analysis. *J. Great Lakes Res.* **2009**, *35*, 272–284. [[CrossRef](#)]
42. Chapra, S.C.; Dolan, D.M. Great Lakes total phosphorus revisited: 2. Mass balance modeling. *J. Great Lakes Res.* **2012**, *38*, 741–754. [[CrossRef](#)]
43. ECCC, Environment and Climate Change Canada, Canadian Environmental Sustainability Indicators: Phosphorus levels in the offshore waters of the Great Lakes. 2020. Available online: www.canada.ca/en/environment-climate-change/services/environmental-indicators/phosphoruslevels-off-shore-great-lakes.html (accessed on 12 December 2022).
44. McKay, R.M.L.; Bullerjahn, G.S.; Porta, D.; Brown, E.T.; Sherrell, R.M.; Smutka, T.M.; Sterner, R.W.; Twiss, M.R.; Wilhelm, S.W. Consideration of the bioavailability of iron in the North American Great Lakes: Development of novel approaches toward understanding iron biogeochemistry. *Aquat. Ecosyst. Health Manag.* **2004**, *7*, 475–490. [[CrossRef](#)]
45. Stoffyn-Egli, P. Conservative Behaviour of Dissolved Lithium in Estuarine Waters. *Estuar. Coast. Shelf Sci.* **1982**, *14*, 577–587. [[CrossRef](#)]
46. Kszos, L.A.; Stewart, A.J. Review of lithium in the aquatic environment: Distribution in the United States, toxicity and case example of groundwater contamination. *Ecotoxicology* **2003**, *12*, 439–447. [[CrossRef](#)]
47. Smith, J.P.; Boyd, T.J.; Cragan, J.; Ward, M.C. Dissolved rubidium to strontium ratio as a conservative tracer for wastewater effluent-sourced contaminant inputs near a major urban wastewater treatment plant. *Water Res.* **2021**, *205*, 117691. [[CrossRef](#)]
48. Johannesson, K.H.; Lyons, W.B.; Stetzenbach, K.J.; Byrne, R.H. The solubility control of rare earth elements in natural terrestrial waters and the significance of PO_4^{3-} and CO_3^{2-} in limiting dissolved rare earth concentrations: A review of recent information. *Aquat. Geochem.* **1995**, *1*, 157–173. [[CrossRef](#)]
49. Byrne, R.H.; Kim, K.-H. Rare earth element scavenging in seawater. *Geochim. Et Cosmochim. Acta* **1990**, *54*, 2645–2656. [[CrossRef](#)]
50. Hayhoe, K.; VanDorn, J.; Croley, T.; Schlegal, N.; Wuebbles, D. Regional climate change projections for Chicago and the US Great Lakes. *J. Great Lakes Res.* **2010**, *36*, 7–21. [[CrossRef](#)]
51. Byun, K.; Hamlet, A.F. Projected changes in future climate over the Midwest and Great Lakes region using downscaled CMIP5 ensembles. *Int. J. Climatol.* **2018**, *38*, e5310553. [[CrossRef](#)]
52. Correll, D.L. The Role of Phosphorus in the Eutrophication of Receiving Waters: A Review. *J. Environ. Qual.* **1998**, *27*, 261–266. [[CrossRef](#)]

Disclaimer/Publisher’s Note: The statements, opinions and data contained in all publications are solely those of the individual author(s) and contributor(s) and not of MDPI and/or the editor(s). MDPI and/or the editor(s) disclaim responsibility for any injury to people or property resulting from any ideas, methods, instructions or products referred to in the content.